Global and Local Approaches of Creep Crack Initiation and Growth Applied to an Austenitic Stainless Steel and an Aluminum Alloy

R. PIQUES and A. PINEAU

Centre des Matériaux — Ecole des Mines, B.P.87 — 91003 Evry — Cédex, France UA CNRS N°866

ABSTRACT

Both the initiation and the propagation of creep cracks have been studied in a creep ductile material (Austenitic stainless steel) and in a creep-brittle material (2219 Al alloy). There exists no unique correlation with global parameters (K or C*) for all the stages of creep cracking, especially creep crack growth. A local approach is developed to circumvent these limitations. In this approach the crack tip stress-strain field is calculated using either the results of finite element calculations or the theoretical results obtained from the application of fracture mechanics to creeping solids. Damage laws are obtained from tests carried out on notched specimens. In 2219 Al alloy this damage law is obtained from the application of continuum damage mechanics. In stainless steel, the damage law is based on measurement of intergranular damage.

KEYWORDS

Creep crack initiation, Creep crack growth, Viscoplasticity, Viscoplastic Fracture Mechanics, Finite element analysis, Creep damage, Austenitic stainless steel, 2219 Al alloy.

INTRODUCTION

A large number of studies have been devoted to high temperature cracking. In particular creep cracking has been extensively studied in structural materials, such as stainless steels, low alloy steels, Ni-base superalloys and Al alloys (For a review, see eg. Pineau, 1987; Bensussan, 1986, 1987; Diboine, 1987; Maas, 1985). In these studies the emphasis was laid essentially upon creep crack growth (CCG) and not creep crack initiation (CCI) although this latter stage can represent a large part of the lifetime of cracked components. The first aim of the present work is to provide data concerned not only with CCG behavior but also with CCI behavior in two structural materials : an austenitic stainless steel and an aluminum alloy.

Several approaches are possible. It is convenient to divide these approaches into two main types. The "global approach" results directly from the extension of Fracture Mechanics to creeping solids (Riedel and Rice, 1980, 1981). It is assumed that the fracture resistance can be described in terms of a unique global parameter, which is K for creep brittle materials

or C* parameter for creep ductile materials. For materials which creep by secondary power law creep only, a transition time, t_{tr} between small and large-scale creep conditions has been introduced. For $t \ll t_{tr}$ and $t \gg t_{tr}$, respectively, the crack-tip stress field is given for $r \rightarrow o$ by singularities fully determined either by K or by C*. The materials used in the present study can be classified as : creep ductile for austenitic stainless steel and creep brittle for the aluminum alloy. The load-geometry parameters which are assumed to describe their CCI and CCG behaviors are therefore C* or K, respectively.

Another approach relies upon the fact that it is possible to model macroscopic fracture behavior in terms of local fracture criteria which are derived either from the continuum damage mechanics or from microstructural observations. This is the "local approach". Actually, in many cases, the two approaches are more complementary than contradictory in the sense that the analytical stress-strain field derived from the fracture mechanics of creeping solids is used to calculate the accumulation of creep damage ahead of the crack tip. In the present paper, this is the solution which was adopted to model CCG behavior of stainless steel. However fully numerical calculations based on the finite element method can also be used to model the crack tip stress strain field. In the present work this solution was used for the aluminum alloy. The methodology used in the latter approach relies upon tests and calculations performed not only on cracked specimens but also on notched specimens to derive a damage law, under an incremental form, in which the effect of the relevant components of the stress and/or strain tensor are taken into account.

EXPERIMENTAL PROCEDURES

The composition of the austenitic stainless steel (0.02C - 0.077N - 17.3Cr - 12.5Ni - 2.44Mo) and its mechanical properties, including tensile properties, primary and stationary creep laws are given in detail elsewhere (Bensussan et al., 1986). The composition of the 2219-T851 aluminum alloy (6.3Cu-0.3Mn-0.18Zr), its tensile properties and its stationary creep law determined at 175°C are also reported elsewhere (Bensussan, 1986).

Tests on notched round bars containing a notch with either a 5 mm root radius (FLE5) or a 1 mm root radius (FLE1) were carried out on both materials. The details about the experimental procedures are given elsewhere (Levaillant et al., 1985; Yoshida et al., 1986; Yoshida et al., 1987). In addition creep cracking tests were carried out on stainless steel over the temperature range between 575 and 650°C using different types of specimens, including not only conventional CT specimen, double edge notched (DEN) specimens but also axisymmetrically cracked (AX) specimens. Full details about these tests are given elsewhere (Maas et al., 1984; Maas, 1984; Piques, 1987; Bensussan et al., 1988). The Al alloy was tested at 175°C using CT type specimens (Bensussan et al., 1988). All these specimens were fatigue precracked at room temperature before being tested at elevated temperature under constant load, except otherwise stated. In the creep tests, the crack length a(t) was measured using a D.C. potential drop technique. Load-line displacement $\delta(t)$ was recorded using extensometers. CCI time, T_i, was defined for stainless steel as the time necessary for the initial crack to propagate over a critical distance $X_c = 50$ µm ($\simeq$ grain size). In the case of 2219 alloy it was prefered to define T_i as the time necessary for the potential drop output voltage to increase 1 %, which corresponds to $X_c = 100$ to 180µm depending on the initial crack length.

K was calculated using the solutions available from the literature. For the definition of C* parameter we used an "experimental" estimation according to Harper and Ellison method (1977) for CT specimen based on the measured load-line displacement rate $\dot{\Delta}_{exp}$, ie $C^* \simeq P\dot{\Delta}_{exp}/BW$. A similar expression was used for AX type specimens (Bensussan et al., 1986).

RESULTS AND DISCUSSION

Creep Cracking Behavior

The results of creep crack initiation are given in Fig.1 and 2, for 2219 alloy and austenitic stainless steel, respectively.In the latter case, a wide range of conditions (temperature, specimen geometries, initial crack lengths) were used. In both cases a unique correlation appears to exist between T_i and K for 2219 Al alloy and between T_i and C^*_{exp}, for stainless steel. These correlations can be expressed as :

- For 2219 Al alloy, at 175°C, $T_i K^8 =$ Constant (1)
- For Stainless Steel, between 575-650°C, $T_i C^{*0,65}_{exp} =$ Constant (2)

The results of CCG rate tests on 2219 Al alloy are shown in Fig.3. More data are given elsewhere (Bensussan et al., 1988) . Here we have only included the results of four typical tests obtained under constant load, i.e under increasing K. A typical two-stage behavior is observed when the CCG rate is plotted versus K. A stage I regime corresponding to low CCG rates is firstly observed. This regime is strongly dependent on the initial conditions. There exists no unique correlation between da/dt and K. On the other hand, the stage II CCG rates ($da/dt \gtrsim 10^3$ µm/h) were found to be independent of the initial K and to depend only on the instantaneous value of K. This conclusion applies if a scatter band in da/dt of about 3 is accepted. The validity of this conclusion was reinforced by the results of further tests performed under decreasing K. The results of such a test are included in Fig.3. The specimen was firstly subjected to a constant load (increasing K) and, then, to a constant displacement (decreasing K), when the stage II crack growth regime was reached. These results strongly suggest that in this material a steady or quasi-steady state can be reached in the stage II regime. In this regime a unique correlation between da/dt and K can be established :

$$da/dt = A\,K^4 \qquad (3)$$

The fact that in this material creep damage was observed to be very localized around the crack tip might explain why a steady-state regime of CCG can be established. However the transient regime cannot be simply described using a single parameter, such as K.

The results of CCG rate tests on stainless steel are shown in Fig.4. In this figure we have only included the results of typical tests performed on CT specimens (For more detail, see Piques et al., 1987). In this material a two-stage regime is also observed when da/dt is plotted versus C^*_{exp}. The stage I regime ($da/dt \lesssim 1$ µm/h) is strongly dependent on the initial conditions. The width of the scatter band in stage II is considerable. However in this latter regime, as noticed by other authors (see eg Taira et al., 1979) it appears that, within a first approximation, the CCG rate is

proportional to C^*_{exp}. It has already been shown that this proportionality reduces to a trivial correlation between da/dt and da/dt (Bensussan et al., 1986). This is due to the fact that, at large da/dt, most of the variations of $\dot{\delta}_{exp}$ are due to the creep crack extension and not to the overall creep deformation taking place within the cracked specimens. These results therefore show that, in stainless steel, it is impossible to correlate the CCG rates with a unique parameter such as C*. In this material CCG behavior is strongly history dependent. This might be related to the fact that the observed creep damage was found to spread over large distances ahead of the crack tip.

Creep Damage Laws

For both materials creep damage laws were established from creep rupture tests carried out on notched specimens. Austenitic stainless steel was investigated more thoroughly (Yoshida et al.1987). Here only a short account of the results is given to illustrate the method used to develop these laws. Fig.5 shows the variation of the maximum principal stress, σ_{zz} (parallel to the specimen axis) in the minimum section of the specimen as a function of time. These results were obtained on one specific geometry (FLE1) subjected either to a low nominal stress (330 MPa) leading to a time to failure $t_R \simeq$ 13000 hours (Fig.5a) or to a larger nominal stress (404 MPa, $t_R \simeq$ 400 hours). In the latter case, it was observed that intergranular fracture occurred preferentially in the vicinity of the notch throat where σ_{zz} remains maximum for a significant period of time before failure. On the other hand, it was observed that intergranular fracture took place in the center of the specimen subjected to a lower stress (330 MPa). This fractographic observation correlates well with the calculated stress distribution shown in Fig.5a. Intergranular damage, D_I was measured using quantitative metallography. D_I was defined as the relative ratio of the length of cracked grain boundaries measured on a unit section.The damage evolution law was written as :

$$dD_I = A \langle \Sigma \rangle^{\alpha} \epsilon_{eq}^{\beta} d\epsilon_{eq} \qquad (4)$$

where A, α and β are numerical constants, ϵ_{eq} is the equivalent Von-Mises creep strain, while Σ is the maximum principal stress. Moreover in the most deeply notched specimens it was observed that at failure,

$$D_I = D_I^c \simeq 3\%$$

Similar metallographical measurements could not be made in 2219 Al alloy. In this material an empirical damage law derived from continuum damage mechanics was introduced as :

$$\frac{dD}{dt} = \frac{1}{t_D} \left[\frac{\langle \Sigma \rangle^{0.9} \sigma_{eq}^{0.1}}{\sigma_D} \right]^{10} \qquad (5)$$

where t_D and σ_D are numerical constants while σ_{eq} is the equivalent Von-Misès stress. An attempt was made (Contesti et al., 1987) to show how this continuum damage mechanics approach could be used in austenitic stainless steel.

Local Approach of Creep Crack Initiation and Creep Crack Growth.

2219 Al alloy. In a model proposed by Riedel and Rice (1980) CCI was assumed to occur when crack tip creep strains reached a critical value, ϵ_c, over a critical distance, X_c, ahead of the crack. From this one can easily arrive at :

$$K^{2n_2} T_i = f(\epsilon_c) \qquad (6)$$

when crack tip creep strains are calculated using the Riedel and Rice secondary creep singular fields. In the case where ϵ_c is assumed to remain constant an exponent of $2n_2 = 48$ is predicted by this model instead of an experimental value of 8 (Eq.1). This might be attributed to the fact that in this material the short time singular stress field (which does not account for initial plasticity) does not describe accurately the crack tip stresses, as shown by finite element analyses of cracked CT specimens (Bensussan, 1986). These calculations were used to model CCI. Creep damage was computed at the nodes of the finite element mesh according to Eq (5) and to the numerically calculated stresses. Initiation was assumed to take place when D reached a value of 1 in the volume $r \lesssim X_c$ ahead of the crack tip. The results of these simulations are shown in Fig.6, where it is observed that the calculated slope of the T_i-K relation (8) is in good agreement with the experimental slope and that the best results are obtained by taking $X_c = 250\mu m$.

Austenitic stainless steel. It has already been shown that the ductility exhaustion concept in which it is assumed that fracture takes place when the calculated creep strain reaches a critical value, ϵ_c, over a critical distance, X_c was able to model both CCI and CCG behavior (Maas et al., 1985). However this type of material exhibits complex variation of creep ductility, as a function of time, because of the aging effects (Yoshida et al. 1986; Yoshida et al., 1987). Therefore it appears to be preferable to use the results of intergranular damage, D_I in an attempt to model both CCI and CCG. In the present study, only CCG is considered. Moreover for simplification sake we use the results of the theoretical crack tip stress-strain field (Riedel and Rice, 1980, 1981). Finite element calculations showed that in a CT type specimen this theoretical asymptotic field was relatively well verified at distances ahead of the crack tip larger than about 50 μm (Bensussan et al., 1986). Furthermore it was observed that close to the crack tip the stress distribution corresponded rapidly either to the primary or stationary creep stabilized stage. These results therefore indicate that a simplified model can be developed in which the RR stationary analytical stress field is used in relation with Eq.(4) to calculate intergranular damage D_I. To model crack growth it is necessary to take into account damage accumulation ahead of a growing crack as in the approach based on ductility exhaustion concept (Maas et al., 1985 and Kubo et al., 1979). Thus, simply stated , the observed acceleration in CCG rate (see Fig.4) is attributed to the accumulation of intergranular creep damage. In Fig.7 we have reported the calculated CCG curves for one specific example. These curves are plotted using a non dimensional form where the crack increment Δa is normalized by the critical distance X_c and the time by T_i. A good agreement is observed between the calculated crack growth curve and the experimental results when the crack tip stress-field is modelled with the RR stationary field. A better agreement is also obtained by taking intergranular damage as a damage parameter instead of

creep ductility. However this difference is not considered to be crucial. The most important result lies in the fact that it appears to be possible to simulate reasonably well the CCG behavior using a local approach. This approach is fully predictive if the experimental T_i - C* correlation is accepted. This first step is necessary to initialize the numerical calculations. Then the values of C* parameter can be calculated using either finite computations (see eg.Hollstein et al., 1987), or, as shown recently, a simplified method based on reference stress and reference length concepts (Piques et al. 1987). In this approach the crack growth rates curves are modelled as successive steps of initiation events taking place over a critical distance X_c = 50 µm when the calculated intergranular damage reaches a critical value D_i^c = 3%, by using an iterative method.

CONCLUSIONS

1. Global load geometry parameters derived from Fracture Mechanics of creeping solids (K or C*) appear to provide unique correlations only with the time to initiation, T_i and not with all the observed stages of creep crack growth. This conclusion applies in particular to the regime of low creep crack growth rates (Stage I) observed in both materials. On the other hand there exists a steady stage regime in 2219 Al alloy in which the creep crack growth rates correlate with K.
2. Fully predictive local approach models of creep crack initiation in 2219 Al alloy and creep crack growth in austenitic stainless steel have been shown to provide convenient means to circumvent the limitations of the empirical correlations which are proposed in the literature between creep cracking behavior and a global load geometry parameter.
3. Global and local approaches of creep cracking are more complementary than contradictory. In particular in austenitic stainless steel an approach based on intergranular damage calculated from an empirical law established on notched specimens, on the one hand, and from the theoretical stress-strain field derived from the fracture mechanics of creeping solids, on the other hand, has been developed.

REFERENCES

Bensussan, P., (February 1986). Thèse de Doctorat-ès-Sciences, Université de Paris Sud-Orsay, France.

Bensussan, P., R. Piques, and A. Pineau, (October 6-8, 1986). Third International Symposium on Nonlinear Fracture Mechanics, Knoxville Tennessee.

Bensussan, P., (October 13-15, 1987). International Seminar on High Temperature Fracture Mechanisms and Mechanics, Dourdan, France.

Bensussan, P., E. Maas, R. Pelloux, and A. Pineau, (1988). *Jal of Pressure Vessel Technology*, 110, pp.42-50.

Contesti, E., G. Cailletaud, C. Levaillant, (1987). *Jal of Pressure Vessel Technology*, 109, pp.228-235.

Diboine, A. and A. Pineau, (1987). *Fatigue Fract. Engng. Mater. Struct.*, 10, pp.141-151.

Harper, M.P. and E.G. Ellison, (1977). *J. Strain analysis*, 12, pp.167-179.

Hollstein, T., R. Kiengler, (October 13-15, 1987). International Seminar on High Temperature Fracture Mechanisms and Mechanics, Dourdan, France.

Kubo, S., S.K. Ohji and X. Ogura, (1979). *Eng. Fract. Mechanics*, 11 1979, pp.315-329.

Levaillant, C., A. Pineau, M. Yoshida, and R. Piques, (1985). Techniques for Multiaxial Creep Testing, Leatherhead, pp.199-208.

Maas, E. and A. Pineau, (1984). Mechanical Behaviour of Materials - IV, ICM4, J. Carlsson and Ohlson, N.G., eds., *Pergamon press*, Oxford, England, 2, pp.763-769.

Maas, E. (in French), (April 1984). Thèse de Docteur Ingénieur, Ecole Nationale Supérieures des Mines de Paris, Paris, France.

Maas, E. and A. Pineau, (1985). *Engineering Fracture Mechanics*, 22, pp.307-325.

Pineau, A., (June-6, 1987). Fifth international conference on mechanical behaviour of materials, Beijing (China).

Piques, R.,P. Bensussan and A. Pineau,(October 1-15 1987) International Seminar on High Temperature Fracture Mechanisms and Mechanics.

Riedel, H. and J.R. Rice, (1980). *Fracture Mechanics ASTM STP* 700, pp.112-130.

Riedel, H., (1981). *Jal Mech. Phys. Solids*, 29, pp.35-49.

Taira, S., R. Ohtani and T. Kitamura, (1979). *Jal Engineering Materials and Technology, Trans. ASME*, 101, pp.154-161.

Yoshida, M., C. Levaillant, A. Pineau, (1986).International Conference on Creep, Tokyo, pp.327-332.

Yoshida, M., C. Levaillant, R. Piques and A. Pineau, (1987). International Seminar on High Temperature Fracture Mechanisms and Mechanics, October 13-15, Dourdan, France.

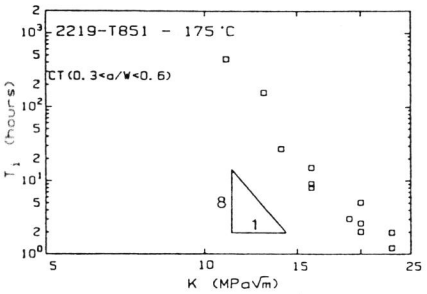

Figure 1 - Time to initiation T_i versus K in 2219-T851 at 175°C.

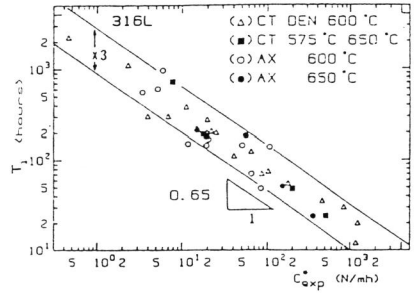

Figure 2 - Time to initiation T_i versus C^*_{exp} in 316L.

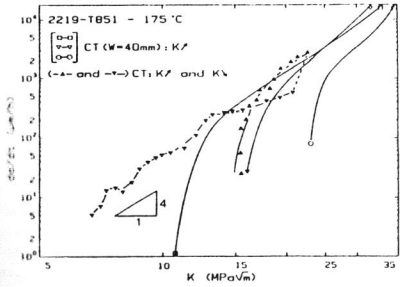

Figure 3 - Creep crack growth rates in 2219-T851 alloy at 175°C.

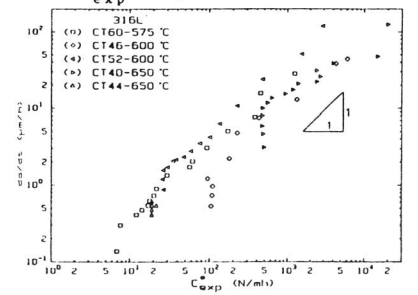

Figure 4 - Creep crack growth rates in 316L at 575°C, 600°C and 650°C.

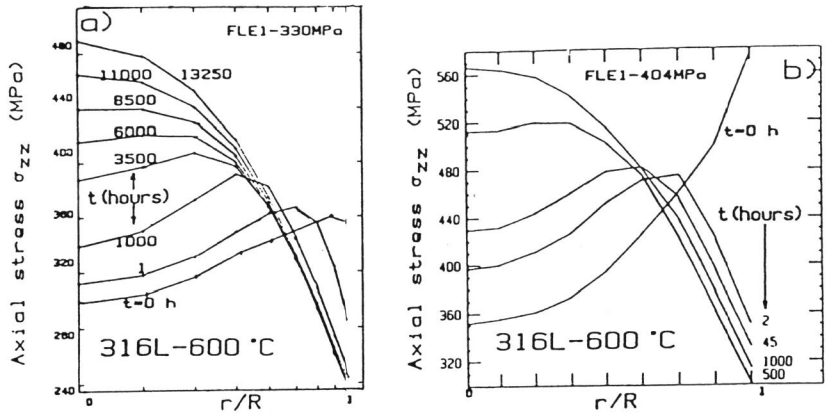

Figure 5 - Radial distribution of axial stress in FLE1 specimen.
a) σ_{nom} = 330 MPa; b) σ_{nom} = 404 MPa.

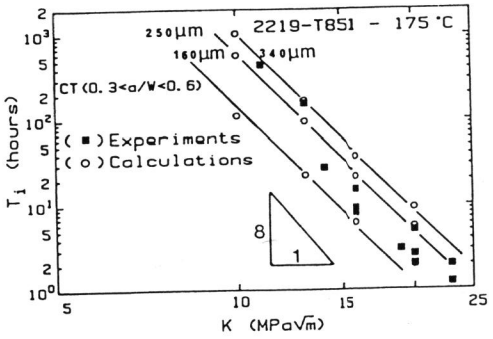

Figure 6 - Comparisons between experimental and calculated times to initiation in 2219-T851 at 175°C.

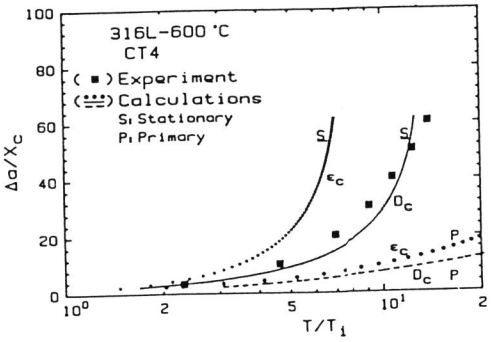

Figure 7 - Comparisons between experimental and calculated creep crack growth curves in 316L at 600°C.